DISCHARGE COEFFICIENTS OF FLAT-FAN NOZZLES

S. L. Post, R. L. Roten, R. J. Connell

ABSTRACT. *The discharge coefficient (C_d) is a measure of how much of the pressure energy of a nozzle is converted into kinetic energy. With the discharge coefficient known, the exit velocity of the liquid sheet from the nozzle can be calculated from the pressure. It is important to be able to accurately calculate this nozzle exit velocity for use in initializing computational simulations such as AGDISP or CFD. The objective of this work was to measure the discharge coefficients for different types of flat-fan nozzles. In this work, a phase-Doppler interferometer was used to measure the exit velocity for standard, pre-orifice, and air-induction flat-fan nozzles, for rated sizes from 01 to 06, at pressures from 1 to 6 bar. From these velocities, discharge coefficients were calculated. The standard flat-fan nozzles had the highest discharge coefficients, while the air-induction nozzles had the lowest discharge coefficients. For a fixed type of nozzle design, the discharge coefficient increased slightly with the rated flow rate. The discharge coefficient decreased slightly with increasing pressure for a given nozzle. Much of the differences in droplet size for different types of nozzles can be explained by atomization theory as a result of the differences in discharge coefficients for the different nozzle designs.*

Keywords. *Atomization, Discharge coefficient, Flat-fan nozzle, Pesticide, Phase Doppler, Sprayers.*

The discharge coefficient of a spray nozzle is a measure of the friction loss in the nozzle as fluid moves through it. It is also a measure of the deviation of the actual flow rate from that predicted by the Bernoulli equation for the same pressure drop across the nozzle. The equation for discharge coefficient is (Post, 2009):

$$Q = C_d A \sqrt{\frac{2\Delta P}{\rho}} \tag{1}$$

where Q is the volume flow rate through the nozzle, A is the exit area of the orifice, ΔP is the pressure drop across the nozzle, and ρ is the density of the fluid being sprayed. Calculating the discharge coefficient with equation 1 requires measurement of the orifice area, which is difficult for the complex geometries of flat-fan nozzles. The orifice area can be eliminated from equation 1 using:

$$Q = AV \tag{2}$$

The discharge coefficient can then be calculated from measurements of the exit velocity:

$$C_d = \frac{V_{exit}}{\sqrt{\frac{2\Delta P}{\rho}}} = \sqrt{\frac{\rho V^2}{2\Delta P}} \tag{3}$$

The maximum possible value of the discharge coefficient is $C_d = 1.0$, which indicates that there was no friction loss in the nozzle and all the pressure energy of the water was converted into kinetic energy. The effective flow area (A_{eff}, mm^2) is defined as:

$$A_{eff} = C_d A \tag{4}$$

The effective flow area should be constant for nozzles of different designs with the same rated flow (i.e., size 02 of standard flat-fan and pre-orifice nozzles). Manufacturers typically do not provide discharge coefficient values. Instead, they provide flow rates for different pressure drops, from which the effective flow area can be inferred. Because pressure and volume flow rate are relatively easy to measure, and usually match the manufacturer's specifications reasonably well (e.g., see the measurements of flow reported by Wang et al., 2015), calculating the discharge coefficient requires one of two more difficult measurements: (1) the geometric outlet area of the nozzle, or (2) the velocity of the liquid sheet exiting the nozzle.

LITERATURE REVIEW

Most of the reported measurements of discharge coefficient reported in the literature are those by Sayinci (2015a, 2015b) and Sayinci and Kara (2015), as well as the measurements by Womac and Bui (2002) and Zhou et al. (1996). In research where droplet velocities have been measured at the location of sheet breakup, such as with PIV, those velocities can be used to calculate the discharge coefficient as well. This includes measurements by Dorr et al. (2013) and Cloeter et al. (2010). Table 1 shows a summary of previously reported values of discharge coefficient for agricultural flat-fan nozzles reported in the literature.

Submitted for review in August 2016 as manuscript number MS 12064; approved for publication by the Machinery Systems Community of ASABE in February 2017. Presented at the 2016 ASABE Annual Meeting as Paper No. 162460834.

The authors are **Scott L. Post, ASABE Member,** Research Scientist, and **Rory L. Roten,** Crop Protection Scientist, Lincoln Agritech, Lincoln, New Zealand; **Robert J. Connell**, Scientist and Independent Researcher, Christchurch, New Zealand. **Corresponding author:** Scott L. Post, Engineering Drive, Lincoln 7640, New Zealand; phone: +64-03-325-3716; e-mail: scott.post@lincolnagritech.co.nz.

Typical discharge coefficients for circular-hole fuel injector nozzles with sharp edges are about 0.80 (ASME, 1961), such as for automobile and diesel fuel injectors. Values reported in the literature for agricultural flat-fan nozzles are much higher, about 0.90 to 0.95, despite the more complex geometry of the elliptical orifice, in which the greater surface area for the same amount of flow area should increase the friction loss. At Reynolds numbers above 2000 (fully turbulent flow), the discharge coefficient is usually constant and does not change with Reynolds number (Lichtarowicz et al., 1965). Cavitation can reduce the value but is not expected to be an issue for the low pressures used in agricultural nozzles. Spikes and Pennington (1959) found that higher discharge coefficients (over 0.90 for non-cavitating flow) could be obtained by chamfering the orifice. Womac and Bui (2002) used a custom-built variable-geometry nozzle that may not be representative of production flat-fan nozzles. Nevertheless, there were some obvious trends in their data, namely that the discharge coefficient increased with orifice exit area. The only previous study of pre-orifice nozzles was that of Sayinci and Kara (2015), who found C_d values of 0.67 to 0.77, as compared to C_d values of 0.91 to 0.94 for standard nozzles.

It is also informative to compare air-induction and conventional flat-fan nozzles of the same flow rating. The measurements of Guler et al. (2007) show how the orifice areas compare for nozzles of the same flow rating and angle (110°) for air-induction (AI) and conventional (XR) nozzles (fig. 1). It can be seen that AI nozzles have larger orifice areas than XR nozzles at the same flow rate, with a nearly linear increase in flow area with flow rate. The AI nozzles have on average 2.27 times the orifice area of the XR nozzles at the same flow rate.

The objective of this work was to calculate the discharge coefficients for three types of commonly used flat-fan nozzles (standard, pre-orifice, and air-induction) on a consistent basis. The data generated can be used in computational models of agricultural spraying and also provide insight into the atomization mechanisms of those nozzles.

Materials and Methods

A phase Doppler interferometer (PDI) probe was used to measure spray velocities directly under the nozzle, as close to sheet breakup as possible. The PDI probe used in this study was a custom-built Demeter probe manufactured by Artium Technologies (Sunnyvale, Cal.). A description of the device is given by Roten et al. (2016), and the theory of operation for Artium devices is provided by Bachalo and Houser (1984). A unique feature of this device is the fixed geometry of the transmitter and receiver, so they do not have to be aligned. The measurements from the PDI depend on the voltage used in the detector (Post et al., 2016); as the voltage is increased, more small droplets are detected. For

Table 1. Summary of values of discharge coefficient reported in the literature for flat-fan nozzles.

Nozzle Type	Reference	Nozzles	Pressure (bar)	C_d	Notes
Standard	Sayinci (2015a)	110-015, 02, 03	1.5 to 10	0.88 to 0.96	Pressure, flow, and nozzle area
	Sayinci (2015b)	110-02, 03, 04, 06	2.0 to 8.0	0.85 to 0.98	Pressure, flow, and nozzle area
	Sayinci and Kara (2015)	120-015, 03, 05	1.5 to 8.0	0.91 to 0.94	Pressure, flow, and nozzle area
	Womac and Bui (2002)	Custom	1.4 to 4.1	0.95	Custom, only for largest opening
	Zhou et al. (1996)	80 and 110	-	0.93	Nozzle area
	Dorr et al. (2013)	110-02	1.5 to 8.0	0.94	PIV velocity measurements
	Cloeter et al. (2010)	80-02	2.76	0.91	PIV velocity measurements
Pre-orifice	Sayinci and Kara (2015)	AD120-015, 03, 04	1.5 to 8.0	0.67 to 0.77	Pressure and nozzle area
Air-induction	Cloeter et al. (2010)	AI95-02	2.76	0.38	PIV velocity measurements
	Dorr et al. (2013)	AI110-015, 02	1.5 to 8.0	0.38 to 0.43	PIV velocity measurements

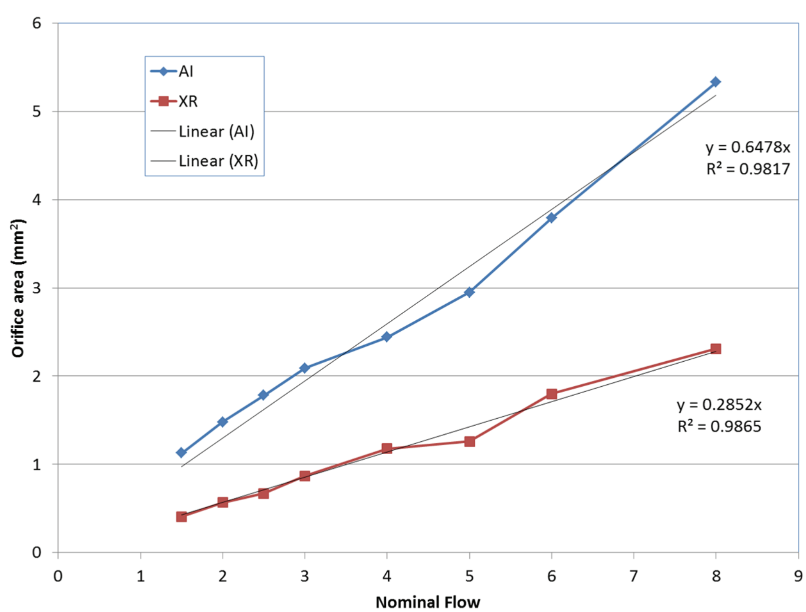

Figure 1. Orifice areas of air-induction (AI) and conventional (XR) flat-fan nozzles (data from Guler et al., 2007).

all measurements, a voltage of 200 V was used, as this voltage gave the peak velocity. Droplet size and flux measurements were not used, as the validation rate for droplet size was quite low, likely due to the droplets having not yet achieved a spherical shape so close to sheet breakup, but the validation rate for the velocity measurements remained high (over 90%). Data were collected until the average velocity stabilized to within 1%. This was typically 10,000 to 50,000 counts.

The water spray system included a 12 V pump (7 L min^{-1}, 8.27 bar, Smoothflo model DDP-552, Aquatec Water Systems, Inc., Irvine, Cal.) connected to a single nozzle body with a flat-fan nozzle and check valve type strainer with size 50 mesh to assist the rate at which the plume formed and to promote accuracy (strainer model 4193A-PP, Teejet Spraying Systems, Wheaton, Ill.). The pump could provide a maximum pressure of 6.20 bar (90 psi) for a small (01 size) nozzle, with the maximum obtainable pressure decreasing as the nozzle size increased.

All measurements were made with stationary nozzles in a lab setting. Average velocities are reported. The PDI had a limited range of droplet sizes, as it was designed for drift measurements and therefore was not suitable for characterizing the full droplet size distribution from air-induction and large nozzle sprays. The PDI can be used as a laser-Doppler velocimeter (LDV), which should be independent of droplet size. The probe design allowed close placement near the nozzle. We placed the PDI as close to the nozzle exit as possible (8 mm for conventional nozzles, 23 mm for air-induction nozzles) where the liquid sheet started to breakup and the PDI could acquire velocity measurements (fig. 2) that were nearly equal to the sheet velocity coming out of the nozzle before entrainment of ambient air began to reduce the droplet velocities. The different nozzle types have different lengths for sheet breakup and hence required different measurement locations. This was found by moving the nozzle vertically above a fixed PDI location to find the point closest to the nozzle at which reliable measurements could be made. Because the air-induction nozzles had a wider orifice slot, the liquid sheet was thicker and took longer to break up.

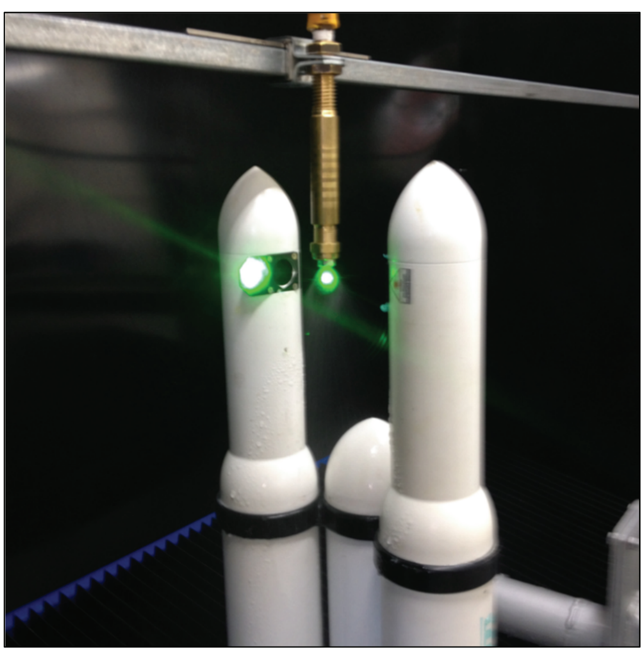

Figure 2. Demeter PDI showing laser beam intersection immediately below nozzle orifice.

Stainless steel standard flat-fan nozzles (sizes 110-01, 110-03, and 110-06), pre-orifice nozzles (sizes 80-015, 80-03, and 80-05), and air-induction nozzles (sizes 110-015, 110-02, 110-025, and 110-04) were used in this study. All nozzles were Teejet brand. Occasional clogging of the smallest (01 size) nozzles was an issue.

The primary safety hazard in conducting the experiments was the possibility of reflected laser light entering the operator's eye. To mitigate against that hazard, the operator wore laser safety goggles that blocked the wavelength of light used by the PDI probe. A different design of the beam dump on the PDI could also reduce the risk of laser exposure. All of the water sprayed was collected in a closed-loop system to prevent accumulation of water in puddles on the floor and eliminate the possibility of slipping hazards.

RESULTS

Table 2 shows the measured velocities at sheet breakup for the standard 110-01 nozzle. The theoretical discharge velocity was calculated from the Bernoulli equation:

$$V = \sqrt{\frac{2\Delta P}{\rho}} \tag{5}$$

In all cases, the Reynolds number was 5000 or higher, so fully turbulent flow can be assumed. The discharge coefficient (C_d) was calculated as the ratio of the measured nozzle exit velocity ($V_{measured}$) to the theoretical nozzle exit velocity ($V_{theoretical}$). For example, for the 110-01 nozzle at 2.07 kPa (30 psi), C_d = (18.4 m s^{-1}) / (20.3 m s^{-1}) = 0.90.

Figure 3 shows the variation of discharge coefficient with operating pressure for the standard flat-fan nozzles, using the data from table 3. Tables 4 and 5 show the calculated discharge coefficients for pre-orifice and air-induction nozzles, respectively. All discharge coefficients are average values. Repeatability of velocity measurements, and hence discharge coefficients, was typically within ±1% for measurements with the same nozzle, and nozzle-to-nozzle variations for different nozzles of the same type and flow rate were also within ±1%. Two trends are apparent: the discharge coefficient decreased with increasing pressure and increased with increasing nozzle size; however, these trends were not com-pletely consistent. At pressures of 3 bar (45 psi) and above, the values tended to stabilize around a constant value. With the higher flow rates of larger nozzles, the pump could not provide pressure as high as that provided for the smaller nozzles.

Table 2. Measured velocities and calculated discharge coefficients for standard flat-fan 110-01 nozzle as a function of pressure.

Pressure (kPa)	Pressure (psi)	$V_{theoretical}$ (m s^{-1})	$V_{measured}$ (m s^{-1})	C_d	Reynolds Number
2.07	30	20.3	18.4	0.90	5000
3.10	45	24.9	21.6	0.87	5800
4.14	60	28.8	25.1	0.87	6800
5.17	75	32.2	28.2	0.88	7600
6.20	90	35.2	30.6	0.87	8300

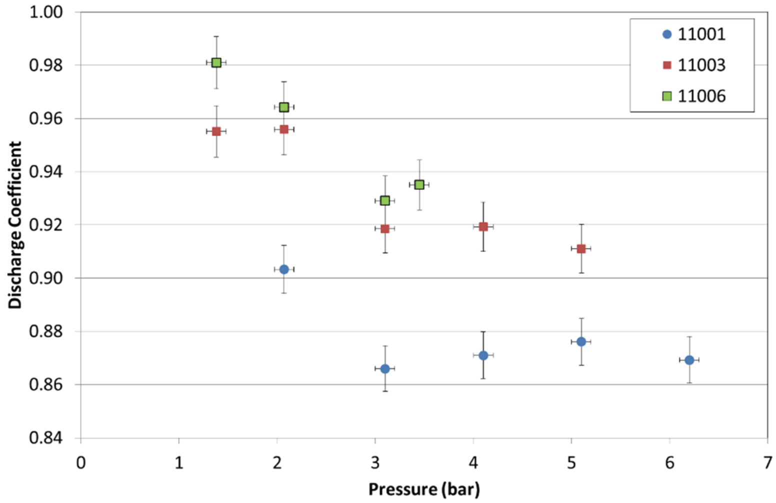

Figure 3. Discharge coefficients calculated from measured velocities and pressures for standard flat-fan nozzles. Error bars represent the uncertainty in the measurements.

Table 3. Discharge coefficients for standard flat-fan nozzles as a function of pressure and nozzle size.

Pressure (kPa)	Pressure (psi)	Standard Flat-Fan Nozzle		
		110-01	110-03	110-06
2.07	30	0.90	0.96	0.96
3.10	45	0.87	0.92	0.93
4.14	60	0.87	0.92	-
5.17	75	0.88	0.91	-

Table 4. Discharge coefficients for pre-orifice flat-fan nozzles as a function of pressure and nozzle size.

Pressure (kPa)	Pressure (psi)	Pre-Orifice Nozzle		
		80-015	80-03	80-05
2.07	30	0.69	0.72	0.73
3.10	45	0.66	0.68	0.69
4.14	60	0.66	0.66	-
5.17	75	0.64	-	-

Table 5. Discharge coefficients for air-induction flat-fan nozzles as a function of pressure and nozzle size.

Pressure (kPa)	Pressure (psi)	Air-Induction Nozzle			
		110-015	110-02	110-025	110-04
2.07	30	0.52	0.54	0.52	0.60
3.10	45	0.53	0.53	0.51	0.57
4.14	60	0.51	0.50	0.51	0.54
5.17	75	0.51	0.50	0.51	-

Table 6. Discharge coefficients for air-induction nozzles with and without surfactant. Values are averaged over all pressures from 2.07 to 5.17 bar.

	Air-Induction Nozzle			
Spray Liquid	110-015	110-02	110-025	110-04
Water	0.52	0.52	0.51	0.57
Surfactant	0.52	0.53	0.51	0.59

All measurements in tables 2 through 5 were made with tap water as the spray liquid. For the air-induction nozzles, we also assessed the effects of the spray liquid formulation on the measured velocity and discharge coefficients. Because the air-induction nozzles have an air-induction port, the amount of air trapped in the spray may depend on the surface tension of the mixture, which in turn could affect the flow properties at the nozzle exit. A surfactant (Superwet 1000, SST Australia Pty Ltd, Bayswater, Victoria, Australia) was used to assess the effects of surface tension on nozzle flow properties. As shown in table 6, there were minimal differences in measured discharge coefficients for the air-induction nozzles with water and with the chosen surfactant solution.We can compare our results with previously reported values in the literature. Sayinci (2015b) reported the same trend of C_d decreasing with increasing pressure (with the exception of when a ball check valve is used). There was no clear trend in his data for change in C_d with orifice size. Overall, the values presented in this study in tables 3 through 5 are comparable to those previously reported in the literature, as shown in table 1, with the exception of the air-induction nozzles, where the values found in this study are higher than those previously reported in the literature. There are two possibilities for this discrepancy: the nozzle types used in the different studies were of significantly different geometrical designs and therefore had different discharge coefficients, or the PIV measurements in the previous studies were not sufficiently close to the nozzle, and the measured velocities were therefore reduced due to mixing and entrainment of air into the spray sheet, so that the measured velocity was less than that of the liquid sheet exiting the nozzle. This is the first published study that compares discharge coefficients for three types of flat-fan nozzles (standard, pre-orifice, and air-induction) using a consistent methodology. The advantage of the phase Doppler velocity measurement technique used in this study is that it does not rely on difficult measurements of the orifice area in the complex geometry of flat-fan nozzles.

Conclusion

The differences in nozzle exit velocities between different flat-fan nozzle designs (standard, pre-orifice, and air-induction), as represented by the non-dimensional discharge coefficient, also provide insights into the atomization processes and drift-reduction potential of pre-orifice and air-induction nozzle designs. Atomization theories relying on aerodynamic breakup mechanisms typically predict that the mean droplet size is inversely proportional to the nozzle exit velocity. It is known that pre-orifice nozzles produce coarser sprays than flat-fan nozzles with corresponding spray angles and rated flow, and that air-induction nozzles produce even coarser sprayers than pre-orifice nozzles. Therefore, it is no surprise that there is an inverse correlation between the discharge coefficient and droplet size. The standard flat-fan nozzles had the largest discharge coefficients and the smallest droplets, the air-induction nozzles had the smallest discharge coefficients and the largest droplets, and the pre-orifice nozzles were in the middle.

The measured pressure is the supply line pressure, or the pressure at the inlet to the nozzle. For pre-orifice and venturi nozzles, the pressure loss inside the nozzle causes the effective pressure at the nozzle exit to be lower than at the inlet. If this intermediate pressure immediately before the nozzle exit could be easily measured and used in equation 3, it is expected that the discharge coefficients calculated with equation 3 would be very similar for the three types of nozzles.

Consistent with previously published results, the discharge coefficient decreases slightly with increasing pressure. Changes in nozzle type (standard, pre-orifice, or air-induction) change the discharge coefficient much more than changes in pressure or nozzle size. This variation in discharge coefficient for different types of nozzles should be accounted for in computational simulations of spray dispersion.

REFERENCES

ASME. (1961). *Flowmeter computational handbook*. New York, NY: American Society of Mechanical Engineers.

Bachalo, W. D., & Houser, M. J. (1984). Phase/Doppler spray analyzer for simultaneous measurements of drop size and velocity distributions. *Optical Eng., 23*(5), 235583. https://dx.doi.org/10.1117/12.7973341

Cloeter, M. D., Qin, K., Patil, P., & Smith, B. (2010). Planar laser induced fluorescence (PLIF) flow visualization applied to agricultural spray nozzles with sheet disintegration: Influence of an oil-in-water emulsion. In *Proc. ILASS-Americas 22nd Annual Conf.* Institute for Liquid Atomization and Spray Systems. Retrieved from http://ilass.org/2/ConferencePapers/ILASS2010-161.pdf

Dorr, G. J., Hewitt, A. J., Adkins, S. W., Hanan, J., Zhang, H., & Noller, B. (2013). A comparison of initial spray characteristics produced by agricultural nozzles. *Crop Prot., 53*, 109-117. http://dx.doi.org/10.1016/j.cropro.2013.06.017

Guler, H., Zhu, H., Ozkan, H. E., Derksen, R. C., Yu, Y., & Krause, C. R. (2007). Spray characteristics and drift reduction potential with air-induction and conventional flat-fan nozzles. *Trans. ASABE, 50*(3), 745-754. https://dx.doi.org/10.13031/2013.23129

Lichtarowicz, A., Duggins, R. K., & Markland, E. (1965). Discharge coefficients for incompressible non-cavitating flow through long orifices. *J. Mech. Eng. Sci., 7*(2), 210-219. https://dx.doi.org/10.1243/JMES_JOUR_1965_007_029_02

Post, S. (2009). *Applied and computational fluid mechanics.* Burlington, MA: Jones and Bartlett Learning.

Post, S. L., Connell, R., & Hewitt, A. (2016). Phase Doppler measurements of mass flux distribution in flat-fan sprays. In *Proc. Intl. Conf. Advances in Pesticide Application.* Warwick, UK: Association of Applied Biologists.

Roten, R. L., Post, S. L., Werner, A., Hewitt, A. J., & Safa, M. (2016). Volumetric validation of mass balance using a computational phase Doppler approach for disc core nozzles. *Crop Prot., 79*, 128-134. http://dx.doi.org/10.1016/j.cropro.2015.10.018

Sayinci, B. (2015a). The influence of strainer types on the flow and droplet velocity characteristics of ceramic flat-fan nozzles. *Turkish J. Agric. Forestry, 39*, 1-15.

Sayinci, B. (2015b). Effect of strainer type, spray pressure, and orifice size on the discharge coefficient of standard flat-fan nozzles. *Turkish J. Agric. Forestry, 39*(5), 692-704. https://dx.doi.org/10.3906/tar-1410-89

Sayinci, B., & Kara, M. (2015). The effects of strainer types on flow characteristics of anti-drift (AD) and multi-range (LU) flat-fan nozzles. *Tarim Bilimleri Dergisi - J. Agric. Sci., 21*(4), 558-571.

Spikes, R. H., & Pennington, G. A. (1959). Discharge coefficient of small submerged orifices. *Proc. Inst. Mech. Eng., 173*(1), 661-674. https://dx.doi.org/10.1243/PIME_PROC_1959_173_055_02

Wang, S., Dorr, G. J., Khashehchi, M., & He, X. (2015). Performance of selected agricultural spray nozzles using particle image velocimetry. *J. Agric. Sci. Tech., 17*(3), 601-613.

Womac, A. R., & Bui, Q. D. (2002). Design and tests of a variable flow fan nozzle. *Trans. ASAE, 45*(2), 287-295. https://dx.doi.org/10.13031/2013.8519

Zhou, Q., Miller, P. C. H., Walklate, P. J., & Thomas, N. H. (1996). Prediction of spray angle from flat fan nozzles. *J. Agric. Eng. Res., 64*(2), 139-148. https://dx.doi.org/10.1006/jaer.1996.0055